Syntheses and Properties of a Series of Oxo-Centered Triruthenium Complexes and Their Bridged Dimers with Isocyanide Ligands at Terminal and Bridging Positions

Ken-ichiro Ota,[†] Hirokazu Sasaki,[†] Taeko Matsui,[†] Tomohiko Hamaguchi,[†] Tadashi Yamaguchi,[†] Tasuku Ito,*[,†] Hiroaki Kido,[‡] and Clifford P. Kubiak[§]

Department of Chemistry, Graduate School of Science, Tohoku University, Sendai 980-8578, Japan, Department of Chemistry, College of Engineering, Nihon University, Koriyama 963-8642, Japan, and Department of Chemistry and Biochemistry, University of California, San Diego, La Jolla, California 92093-0358

Received February 25, 1999

Seven new oxo-centered triruthenium complexes with 2,6-dimethylphenyl isocyanide (CNXy) as a terminal ligand, $[Ru_3(O)(CH_3CO_2)_6(CNXy)_n(L)_{3-n}]$ {L = CO, $n = 2$ (**1**); L = pyridine (py), $n = 1$ (**2**); L = 4-(dimethylamino)-pyridine (dmap), $n = 1$ (**3**); L = py, $n = 2$ (**4**); L = dmap, $n = 2$ (**5**); $n = 3$ (**6**); L = 5-(4-pyridyl)-10,15,20-triphenylporphine, $n = 2$ (**7**)}, three new pyrazine (pz) bridged dimers of triruthenium complexes with terminal isocyanide ligands, $[\{Ru_3(O)(CH_3CO_2)_6(CNXy)_n(L)_{2-n}\}_2(\mu\text{-pz})]$ {L = py, $n = 1$ (**8**); L = dmap, $n = 1$ (**9**); $n = 2$ (**10**)}, and three new 1,4-phenylene diisocyanide bridged dimers, $[\{Ru_3(O)(CH_3CO_2)_6(L)_2\}_2(\mu\text{-}CNC_6H_4NC)]$ {L = py (**11**); L = dmap (**12**); L = CNXy (**13**)}, were prepared. All the $Ru_3(O)$ cluster core in these compounds have the formal oxidation state of $Ru^{III}_2Ru^{II}$ in the isolated state. In contrast to the related carbonyl derivatives, the isocyanide complexes gave triruthenium complexes with more than one isocyanide ligand, reflecting the lower π acidity of isocyanides. In the mixed carbonyl/isocyanide complex $[Ru_3(O)(CH_3CO_2)_6(CO)(CNXy)_2]$ (**1**), the carbonyl and isocyanide ligands compete in π acidity for the $Ru_3(O)$ cluster core, and as a result **1** undergoes a facile elimination of the CO ligand followed by substitution. With use of this reaction, many other triruthenium isocyanide complexes were prepared. Coordination of isocyanide ligands to these triruthenium complexes causes the redox potentials to be shifted anodically relative to the corresponding pyridine derivatives. The pz bridged dimers, **8** and **9**, gave stable one-electron-reduced species which are in the mixed-valence state with respect to the Ru_3 core, as is evidenced by a large redox wave splitting for the $Ru^{III}_2Ru^{II}-pz-Ru^{III}_2Ru^{II}/Ru^{III}_2Ru^{II}-pz-Ru^{III}Ru^{II}_2/Ru^{III}Ru^{II}_2-pz-Ru^{III}Ru^{II}_2$ process ($\Delta E_{1/2} = 349$ mV for **8** and 393 mV for **9**). On the other hand, 1,4-phenylene diisocyanide bridged Ru_3 dimers **11**−**13** gave no stable mixed-valence state, indicating that the electronic communication between the Ru_3 units through this bridge is negligibly small. The compound $[Ru_3(O)(CH_3CO_2)_6(CNXy)(py)_2]$ (**2**) crystallized in the orthorhombic *Pbcn* space group with $a = 18.393(5)$ Å, $b = 14.428(2)$ Å, $c = 17.396(2)$ Å, and $Z = 4$. A comparison of Ru−O(acetate) distances reveals that the site coordinated by the isocyanide ligand is formally Ru(II).

Introduction

The oxo-centered triruthenium cluster bridged by six carboxylate ligands with the general formula of $[Ru_3(O)(CH_3CO_2)_6L_3]^{n+}$ (L = neutral monodentate ligand) affords a versatile class of compounds possessing reversible multistep redox processes.[1−26] The overall charge of these complexes in the isolated state depends on the terminal ligands. It is +1 (Ru^{III}_3) for electron-donating ligands such as pyridine (py) [1−9] or water,[10−13] whereas it is neutral ($Ru^{III}_2Ru^{II}$) for electron-withdrawing or π-acidic ligands such as triphenylphosphine[2,14] and CO.[3,15−17] In general, only one carbonyl ligand will coordinate to these triruthenium clusters to give $[Ru^{III}_2Ru^{II}(O)(RCO_2)_6(CO)(L)_2]$, in which the ruthenium coordinated by carbonyl is formally divalent and the others are trivalent. This proves useful in preparing mixed-ligand triruthenium clusters,

[†] Tohoku University.
[‡] Nihon University.
[§] University of California.

(1) Cannon, R, D.; White, R. P. *Prog. Inorg. Chem.* **1988**, *36*, 195−298.
(2) Spencer, A.; Wilkinson, G. *J. Chem. Soc., Dalton Trans.* **1972**, 1570−1577.
(3) Baumann, J. A.; Salmon, D. J.; Wilson, S. T.; Meyer, T. J.; Hatfield, W. E. *Inorg. Chem.* **1978**, *17*, 3342−3350.
(4) Walsh, J. L.; Baumann, J. A.; Meyer, T. J. *Inorg. Chem.* **1980**, *19*, 2145−2151.
(5) Toma, H. E.; Cunha, C. J.; Cipriano, C. *Inorg. Chim. Acta* **1988**, *154*, 63−66.
(6) Kobayashi, H.; Uryu, N.; Tokiwa, A.; Yamaguchi, T.; Sasaki, Y.; Ito, T. *Bull. Chem. Soc. Jpn.* **1992**, *65*, 198−202.
(7) Imamura, T.; Sumiyoshi, T.; Takahashi, K.; Sasaki, Y. *J. Phys. Chem.* **1993**, *97*, 7786−7791.
(8) Abe, M.; Sasaki, Y.; Nagasawa, A.; Ito, T. *Bull, Chem. Soc. Jpn.* **1992**, *65*, 1411−1414.
(9) Abe, M.; Sasaki, Y.; Yamaguchi, T.; Ito, T. *Bull. Chem. Soc. Jpn.* **1992**, *65*, 1585−1590.
(10) Powell, G.; Richens, D. T.; Bino, A. *Inorg. Chim. Acta* **1995**, *232*, 167−170.
(11) Almog, O.; Bino, A.; Garfinkel-Shweky, D. *Inorg. Chim. Acta* **1993**, *213*, 99−102.
(12) Davis, S.; Drago, R. S. *Inorg. Chem.* **1988**, *27*, 4759−4760.
(13) Bilgrien, C.; Davis, S.; Drago, R. S. *J. Am. Chem. Soc.* **1987**, *109*, 3786−3787.
(14) Cotton, F. A.; Norman, J. G. *Inorg. Chim. Acta* **1972**, *6*, 411−419.
(15) Spencer, A.; Wilkinson, G. *J. Chem. Soc., Dalton Trans.* **1974**, 786−792.
(16) Abe, M.; Sasaki, Y.; Yamada, Y.; Tsukahara, K.; Yano, S.; Yamaguchi, T.; Tominaga, M.; Taniguchi, I.; Ito, T. *Inorg. Chem.* **1996**, *35*, 6724−6734.
(17) Ye, S.; Akutagawa, H.; Uosaki, K.; Sasaki, Y. *Inorg. Chem.* **1995**, *34*, 4527−4528.

10.1021/ic990234n CCC: $18.00
Published on Web 08/19/1999

Chart 1

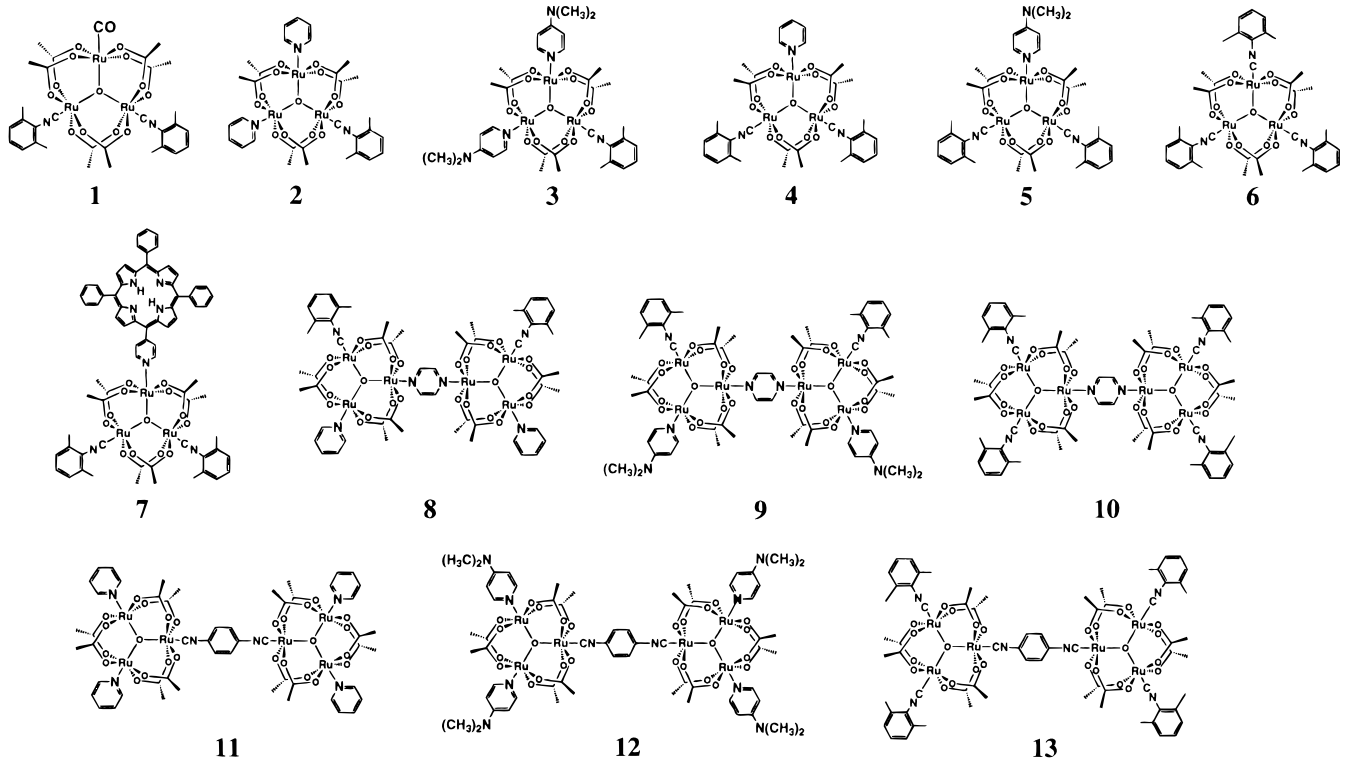

including oligomeric clusters bridged by ligands such as pyrazine (pz)[27−32] and 4,4′-bipyridine,[27,32] since the carbonyl is readily eliminated via chemical oxidation or photolysis.

Isocyanide ligands are isoelectronic with CO and usually form similar complexes. However, in general, isocyanide ligands are considered to be weaker π acids and stronger σ donors than CO. In this study, we have prepared and characterized several new triruthenium cluster complexes with isocyanide ligands. In contrast to the corresponding carbonyl complexes, isocyanides can coordinate to all three terminal ligand sites of these clusters. We have thus synthesized a series of complexes with one to three isocyanide ligands. While investigating these clusters, we found that the triruthenium cluster with one carbonyl and two isocyanide ligands undergoes facile elimination of the carbonyl under ambient conditions. This is quite different reactivity compared to that of the hitherto known carbonyl triruthenium clusters which require photolysis or chemical oxidation to eliminate the carbonyl. By use of this facile substitution reaction, several new compounds including bridged Ru_3 dimers were readily prepared.

The pyrazine bridged dimers of triruthenium clusters containing a carbonyl ligand, $[\{Ru_3(O)(CH_3CO_2)_6(CO)(L)\}_2(\mu\text{-pz})]$, can strongly communicate electronically through the bridging pyrazine. These complexes form strongly interacting charge-transfer complexes when reduced by one electron.[31,32] We also prepared a pyrazine bridged dimer with an isocyanide as a terminal ligand as well as 1,4-phenylene diisocyanide (CNC_6H_4NC) bridged cluster dimers to explore the effects on the interaction between two triruthenium units.

Analogous Ru_3 complexes with methyl isocyanide, $[Ru_3(O)(RCO_2)_6(CH_3NC)_{3-n}(L)_n]$ ($n = 0, 1$; L = H_2O, CH_3OH, py) have been reported by Spencer and Wilkinson, although they were not fully characterized.[15] The complexes prepared in this study are summarized in Chart 1. Hereafter, the following ligand abbreviations will be used: dmap 4-(dimethylamino)pyridine; CNXy, 2,6-dimethylphenyl isocyanide; H_2(4-pyp3p), 5-(4-pyridyl)-10,15,20-triphenylporphine.[33]

Experimental Section

Materials. CH_3CN used in electrochemical measurements was distilled over CaH_2 under a nitrogen atmosphere before use. Tetra-*n*-butylammonium hexafluorophosphate, $[(n\text{-}C_4H_9)_4N]PF_6$, was prepared according to the reported method.[16] Other reagents were used as received.

Measurements. Electronic absorption spectra were recorded on a Shimadzu UV-3100PC spectrometer. ^{1}H NMR spectra were obtained on a JEOL GSX-270 FT NMR spectrometer at 270 MHz. Chemical

(18) Toma, H. E.; Cunha, C. J. *Can. J. Chem.* **1989**, *67*, 1632−1635.
(19) Toma, H. E.; Alexiou, A. D. P. *Electrochim. Acta* **1993**, *38*, 975−980.
(20) Akashi, D.; Kido, H.; Sasaki, Y.; Ito, T. *Chem. Lett.* **1992**, *65*, 143−146.
(21) Cosnier, S.; Deronzier, A.; Llobet, A. *J. Electroanal. Chem. Interfacial Electrochem.* **1990**, *280*, 213−219.
(22) Toma, H. E.; Olive, M. A. L. *Polyhedron* **1994**, *13*, 2647−2652.
(23) Toma, H. E.; Cipriano, C. *Monatsh. Chem.* **1989**, *120*, 815−820.
(24) Toma, H. E.; Santos, P. S.; Cipriano, C. *Spectrosc. Lett.* **1988**, *21*, 909−918.
(25) Toma, H. E.; Matsumoto, F. M.; Cipriano, C. *J. Electroanal. Chem. Interfacial Electrochem.* **1993**, *346*, 261−270.
(26) Abe, M.; Sasaki, Y.; Yamada, Y.; Tsukahara, K.; Yano, S.; Ito, T. *Inorg. Chem.* **1995**, *34*, 4490−4498.
(27) Baumann, J. A.; Salmon, D. J.; Wilson, S. T.; Meyer, T. J. *Inorg. Chem.* **1979**, *18*, 2472−2479.
(28) Wilson, S. T.; Bondurant, R. F.; Meyer, T. J.; Salmon, D. J. *J. Am. Chem. Soc.* **1975**, *97*, 2285−2287.
(29) Baumann, J. A.; Wilson, S. T.; Salmon, D. J.; Hood, P. L.; Meyer, T. J. *J. Am. Chem. Soc.* **1979**, *101*, 2916−2920.
(30) Kido, H.; Nagino, H.; Ito, T. *Chem. Lett.* **1996**, 745−746.
(31) Ito, T.; Hamaguchi, T.; Nagino, H.; Yamaguchi, T.; Washington, J.; Kubiak, C. P. *Science* **1997**, *277*, 660−663.
(32) Ito, T.; Hamaguchi, T.; Nagino, H.; Yamaguchi, T.; Kido, H.; Zavarine, I. S.; Richmond, T.; Washington, J.; Kubiak, C. P. *J. Am. Chem. Soc.* **1999**, *121*, 4625−4632.

(33) We are now studying the photochemistry and photophysics of compound **7**. The results will be published in a separate paper.

Table 1. Crystallographic Data for $[Ru_3(O)(CH_3CO_2)_6(CNXy)(py)_2]\cdot 2CHCl_3$ (**2**·2$CHCl_3$)

empirical formula	$Ru_3O_{13}C_{33}N_3H_{39}Cl_6$
formula weight	1201.61
crystal system	orthorhombic
space group	*Pbcn* (NO. 60)
a (Å)	18.393(5)
b(Å)	14.428(2)
c (Å)	17.396(2)
V(Å^3)	4616(1)
Z	4
D_{calc} (g/cm^3)	1.729
μ(Mo Kα) (cm^{-1})	13.75
radiation (λ (Å))	Mo Kα (0.710 69)
temperature (K)	RT
$2\theta_{max}$ (deg)	55.0
residuals: *R*;[a] R_w[b]	0.031; 0.036

[a] $R = \sum||F_o| - |F_c||/\sum|F_o|$. [b] $R_w = [\sum w(|F_o| - |F_c|)^2/\sum w|F_o|^2]^{1/2}$.

shifts are reported with respect to an internal reference of TMS in $CDCl_3$. Infrared absorption spectra were recorded as KBr pellets on a Jasco IR-810 spectrophotometer.

Cyclic voltammetry (CV) and differential-pulse voltammetry (DPV) were performed using a BAS CV-50W voltammetric analyzer. A glassy carbon electrode was used as the working electrode. The counter electrode was a platinum coil, and the reference electrode was a saturated sodium calomel electrode (SSCE). Solvent used in CV was acetonitrile for Ru_3 monomers and dichloromethane for Ru_3 dimers. CV was performed at a scan rate of 100 mV s^{-1}. All the half-wave potentials $E_{1/2} = (E_{pc} + E_{pa})/2$, where E_{pc} and E_{pa} are the cathodic and anodic peak potentials, respectively, are reported with respect to the SSCE in this study. DPV was performed at a scan rate of 20 mV s^{-1} with a pulse height of 5 mV. Controlled-potential absorption spectra were obtained with an optically transparent thin-layer electrode (OTTLE) cell. The optical path length was 0.5 mm. The working electrode was platinum mesh. The counter electrode was a platinum coil. The reference electrode was an SSCE. Spectroelectrochemical measurements were carried out using a Hokutodenko HA-501 potentiostat. The OTTLE cell was cooled to ca. −10 °C. All electrochemical and spectroelectrochemical measurements were carried out under a nitrogen atmosphere.

X-ray Structural Analysis. Single crystals of $[Ru_3(O)(CH_3CO_2)_6(CNXy)(py)_2]$ (**2**) suitable for X-ray crystallography were obtained by slow recrystallization of **2** in a mixed $CHCl_3$/hexane solution at room temperature. A deep blue prismatic crystal of **2** was attached to the top of a glass fiber and coated with an epoxy resin, and it was then mounted on a Rigaku AFC-7S diffractometer with graphite-monochromated Mo Kα (λ = 0.710 69 Å) radiation. The X-ray data were collected at room temperature, and the $2\theta-\omega$ scan technique was employed. The lattice constants were determined by a least-squares refinement using 25 automatically centered reflections in the range 25° < 2θ < 30°. Three standard reflections were measured every 150 reflections, and they showed no sign of appreciable decay throughout the data collection. The structure was solved by direct methods using the DIRDIF92 PATTY program.[34] All non-hydrogen atoms were located by Fourier synthesis and full-matrix least-squares techniques and refined anisotropically. Crystallographic and other experimental data are listed in Table 1.

Preparations. $[Ru_3(O)(CH_3CO_2)_6(CO)(C_2H_5OH)_2]$,[29] $[Ru_3(O)(CH_3CO_2)_6(CO)(py)_2]$,[30] $[Ru_3(O)(CH_3CO_2)_6(CO)(dmap)_2]$,[35] $[\{Ru_3(O)(CH_3CO_2)_6(CO)(py)\}_2(\mu\text{-pz})]$,[31] $[\{Ru_3(O)(CH_3CO_2)_6(CO)(dmap)\}_2(\mu\text{-pz})]$,[31] and H_2(4-pyp3p)[36] were synthesized according to the reported method.

$[Ru_3(O)(CH_3CO_2)_6(CO)(CNXy)_2]$ (1). To a CH_3OH solution (5 cm^3) of $[Ru_3(O)(CH_3CO_2)_6(CO)(C_2H_5OH)_2]$[29] (100 mg, 0.126 mmol) was added a $CHCl_3$ solution (15 cm^3) of CNXy (33 mg, 0.252 mmol). CO was passed through the solution for 30 min, and then the solution was stirred for 3 h, in which time the color changed from purple to deep blue. The solution was evaporated to dryness using a rotary evaporator, and the residue was dissolved in a minimal amount of $CHCl_3$. The latter solution was placed on a column chromatograph packed with silica gel (Wakogel C-200), and a mixture of $CHCl_3/C_2H_5OH$ (98.5/1.5, v/v) was used as the eluent. The main fraction was collected and evaporated to dryness. The residue was dissolved in a small amount of CH_2Cl_2, and excess *n*-hexane was added to the solution. A deep blue precipitate was collected by filtration. Yield: 65 mg (54%). Anal. Calcd for **1**: C, 38.63; H, 3.76; N, 2.91. Found: C, 38.81; H, 3.92; N, 3.00. ^{1}H NMR in $CDCl_3$: δ 1.90 (6H, acetate methyl), 2.85 (12H, acetate methyl), 3.14 (12H, CNXy methyl), 6.65 (2H, CNXy-*p*), 7.53 (4H, CNXy-*m*). IR (KBr pellet): ν(CO) = 1942 cm^{-1}, ν(CN) = 2150 cm^{-1}. FAB MS: *m*/*z* = 937 (calcd for **1** − CO).

$[Ru_3(O)(CH_3CO_2)_6(CNXy)(py)_2]$ (2). Method 1. To a $CHCl_3$ solution (15 cm^3) of $[Ru_3(O)(CH_3CO_2)_6(CO)(py)_2]$[30] (100 mg, 0.116 mmol) was added CNXy (30 mg, 0.232 mmol), and the solution was refluxed for 1 day, during which time the color changed from violet to deep blue. The solution was evaporated to dryness using a rotary evaporator, and the residue was dissolved in a minimal amount of $CHCl_3$. The latter solution was placed on a column packed with silica gel (Wakogel C-200), and $CHCl_3/C_2H_5OH$ (98.5/1.5, v/v) was used as the eluent. The main fraction was collected and evaporated to dryness. The residue was dissolved in a small amount of $CHCl_3$, and excess *n*-hexane was added to the solution. A deep blue precipitate was collected via filtration. Yield: 27 mg (24%).

Method 2. To a degassed CH_3CN solution (200 cm^3) of $[Ru_3(O)(CH_3CO_2)_6(CO)(py)_2]$[30] (80 mg, 0.093 mmol) was added CNXy (73 mg, 0.558 mmol), and the solution was irradiated for 1 h with a high-pressure Hg lamp. After irradiation, the solution was stirred for 2 h, and the solution color changed from violet to deep blue. The solution was evaporated to dryness with a rotary evaporator, and the residue was dissolved in a minimal amount of $CHCl_3$. The remaining steps were the same as those of method 1. Yield: 43 mg (48%). Anal. Calcd for **2**·2$CHCl_3$: C, 32.99; H, 3.27; N, 3.50. Found: C, 32.85; H, 3.29; N, 3.61. ^{1}H NMR in $CDCl_3$: δ 1.87 (6H, acetate methyl), 2.10 (12H, acetate methyl), 2.76 (6H, CNXy methyl), 7.13 (3H, CNXy benzene ring), 7.99 (4H, py-*m*), 8.15 (2H, py-*p*), 9.26 (4H, py-*o*). IR (KBr pellet): ν(CN) = 2015 cm^{-1}. FAB MS: *m*/*z* = 964 (calcd for **2**).

$[Ru_3(O)(CH_3CO_2)_6(CNXy)(dmap)_2]$ (3). **3** was synthesized by a method similar to that for **2** using $[Ru_3(O)(CH_3CO_2)_6(CO)(dmap)_2]$[35] in place of $[Ru_3(O)(CH_3CO_2)_6(CO)(py)_2]$. Both the methods 1 and 2 for **2** are applicable. Yield: 45%. Anal. Calcd for **3**·$CHCl_3$: C, 37.01; H, 4.14; N, 5.99. Found: C, 37.70; H, 4.17; N, 6.01. ^{1}H NMR in $CDCl_3$: δ 1.82 (6H, acetate methyl), 2.05 (12H, acetate methyl), 2.78 (6H, CNXy methyl), 3.36 (12H, dmap methyl), 7.09 (3H, CNXy benzene ring), 7.20 (4H, dmap-*m*), 9.15 (4H, dmap-*o*). IR (KBr pellet): ν(CN) = 2020 cm^{-1}. FAB MS: *m*/*z* = 1050 (calcd for **3**).

$[Ru_3(O)(CH_3CO_2)_6(CNXy)_2(py)]$ (4). To a $CHCl_3$ solution (20 cm^3) of **1** (70 mg, 0.073 mmol) was added py (6 mg, 0.073 mmol), and the solution was stirred for 1 day. The solution was evaporated to dryness using a rotary evaporator, and the residue was dissolved in a minimal amount of $CHCl_3$. The latter solution was placed on a column packed with silica gel (Wakogel C-200), and a mixture of $CHCl_3/C_2H_5OH$ (98.5/1.5, v/v) was used as the eluent. The main fraction was collected and evaporated to dryness. The residue was dissolved in a small amount of $CHCl_3$, and excess *n*-hexane was added to the solution. A deep blue precipitate was isolated by filtration. Yield: 42 mg (57%). Anal. Calcd for **4**: C, 41.42; H, 4.07; N, 4.14. Found: C, 41.35; H, 4.01; N, 4.12. ^{1}H NMR in $CDCl_3$: δ 2.13 (12H, acetate methyl), 2.22 (6H, acetate methyl), 2.77 (12H, CNXy methyl), 7.20 (6H, CNXy benzene ring), 7.95 (3H, py-*m*+*p*), 8.73 (2H, py-*o*). IR (KBr pellet): ν(CN) = 2060 cm^{-1}. FAB MS: *m*/*z* = 1017 (calcd for **4**).

$[Ru_3(O)(CH_3CO_2)_6(CNXy)_2(dmap)]$ (5). **5** was synthesized by a method similar to that for **4** using dmap in place of py. Yield: 70%. Anal. Calcd for **5**: C, 42.00; H, 4.38; N, 5.30. Found: C, 41.85; H, 4.19; N, 5.13. ^{1}H NMR in $CDCl_3$: δ 2.12 (12H, acetate methyl), 2.19 (6H, acetate methyl), 2.76 (12H, CNXy methyl), 3.36 (6H, dmap

(34) Beurskens, P. T.; Admiraal, G.; Beurskens, G.; Bosman, W. P.; Garcia-Granda, S.; Gould, R. O.; Smits, J. M. M.; Smykalla, C. *The DIRDIF program system*; Technical Report of the Crystallography Laboratory, University of Nijmegen: Nijmegen, The Netherlands, 1992.
(35) Nagino, H. M. S. Thesis, Tohoku University, Sendai, Japan, 1995.
(36) Fleischer, E. B.; Shachter, A. M. *Inorg. Chem.* **1991**, *30*, 3763−3769.

methyl), 7.14 (6H, CNXy benzene ring), 7.22 (2H, dmap-*m*), 8.73 (2H, dmap-*o*). IR (KBr pellet): ν(CN) = 2060 cm^{-1}. FAB MS: *m*/*z* = 1059 (calcd for **5**).

[Ru$_3$(O)(CH$_3$CO$_2$)$_6$(CNXy)$_3$] (6). To a $CHCl_3$ solution (20 cm^3) of [Ru$_3$(O)(CH$_3$CO$_2$)$_6$(CO)(C$_2$H$_5$OH)$_2$][29] (200 mg, 0.252 mmol) was added CNXy (99 mg, 0.756 mmol), and the solution was stirred for 1 day, during which time the color changed from purple to blue-green. The solution was evaporated to dryness with a rotary evaporator, and the residue was dissolved in a minimal amount of $CHCl_3$. The latter solution was placed on a column packed with silica gel (Wakogel C-200), and $CHCl_3/C_2H_5OH$ (98.0/2.0, v/v) was used as the eluent. The main fraction was collected and evaporated to dryness. The residue was dissolved in a small amount of $CHCl_3$, and excess *n*-hexane was added to the solution. A yellow-green precipitate was collected by filtration. Yield: 226 mg (84%). Anal. Calcd for **6**: C, 43.90; H, 4.25; N, 3.94. Found: C, 43.95; H, 4.40; N, 4.03. ^{1}H NMR in $CDCl_3$: δ 2.21 (18H, acetate methyl), 2.82 (18H, CNXy methyl), 7.04 (3H, CNXy-*p*), 7.28 (6H, CNXy-*m*). IR (KBr pellet): ν(CN) = 2100 cm^{-1}. FAB MS: *m*/*z* = 1068 (calcd for **6**).

[Ru$_3$(O)(CH$_3$CO$_2$)$_6$(CNXy)$_2${H$_2$(4-pyp3p)}] (7). To a CH_2Cl_2 solution (20 cm^3) of **1** (78 mg, 0.081 mmol) was added H$_2$(4-pyp3p) (50 mg, 0.081 mmol), and the solution was stirred for 1 day, resulting in a color change from blue-green to brown. The solution was evaporated to dryness using a rotary evaporator, and the residue was dissolved in a minimal amount of $CHCl_3$. The latter solution was placed on a column packed with silica gel (Wakogel C-200), and $CHCl_3/C_2H_5OH$ (98.5/1.5, v/v) was used as the eluent. The main fraction was collected and evaporated to dryness. A $CHCl_3$ solution of the crude product was subjected again to column chromatography (Bio-Beads S-X3). The main fraction was collected and evaporated to dryness. The residue was dissolved in a small amount of $CHCl_3$, and excess *n*-hexane was added to the solution. A purple precipitate was isolated. Yield: 60 mg (48%). Anal. Calcd for **7**·$^1/_5$CH$_2$Cl$_2$: C, 55.81; H, 4.17; N, 6.22. Found: C, 55.81; H, 4.26; N, 6.20. ^{1}H NMR in $CDCl_3$: δ 2.27 (6H, acetate methyl), 2.29 (12H, acetate methyl), 2.81 (12H, isocyanide methyl), 7.17 (2H, CNXy-*p*), 7.24 (4H, CNXy-*m*), 7.81 (9H, Ph-*m*,*m*′,*p*,*p*′), 8.28 (6H, Ph-*o*,*o*′), 8.83 (2H, pyrrole-Ph), 8.90 (4H, pyrrole-Ph-Ph), 9.03 (2H, pyrrole-py), 9.21 (2H, py-*m*), 9.29 (2H, py-*o*). IR (KBr pellet): ν(CN) = 2100 cm^{-1}. FAB MS: *m*/*z* = 1553 (calcd for **7**).

[{Ru$_3$(O)(CH$_3$CO$_2$)$_6$(CNXy)(py)}$_2$(μ-pz)] (8). To a degassed CH_3CN solution (200 cm^3) of [{Ru$_3$(O)(CH$_3$CO$_2$)$_6$(CO)(py)}$_2$(μ-pz)][31] (75 mg, 0.046 mmol) was added CNXy (72 mg, 0.552 mmol), and the solution was irradiated for 1 h with a high-pressure Hg lamp. After irradiation, the solution was stirred for 2 h. The solution was evaporated to dryness using a rotary evaporator, and the residue was dissolved in a minimal amount of $CHCl_3$. The latter solution was placed on a column packed with silica gel (Wakogel C-200), and $CHCl_3/C_2H_5OH$ (98.5/1.5, v/v) was used as the eluent. The main fraction was collected and evaporated to dryness. The residue was dissolved in a small amount of $CHCl_3$, and excess *n*-hexane was added. A blue-green precipitate was collected by filtration. Yield: 39 mg (46%). Anal. Calcd for **8**·$CHCl_3$: C, 34.81; H, 3.54; N, 4.27. Found: C, 34.96; H, 3.68; N, 4.46. ^{1}H NMR in $CDCl_3$: δ 2.02 (12H, acetate methyl), 2.11 (12H, acetate methyl), 2.21 (12H, acetate methyl), 2.77 (12H, CNXy methyl), 7.15 (6H, CNXy benzene ring), 8.02 (4H, py-*m*), 8.13 (2H, py-*p*), 9.2 (4H, py-*o*), 9.28 (4H, pz). IR (KBr pellet): ν(CN) = 2025 cm^{-1}. FAB MS: *m*/*z* = 1846 (calcd for **8**).

[{Ru$_3$(O)(CH$_3$CO$_2$)$_6$(CNXy)(dmap)}$_2$(μ-pz)] (9). 9 was synthesized by a method similar to that for **8** using [{Ru$_3$(O)(CH$_3$CO$_2$)$_6$(CO)(dmap)}$_2$(μ-pz)][31] in place of [{Ru$_3$(O)(CH$_3$CO$_2$)$_6$(CO)(py)}$_2$(μ-pz)]. Yield: 46%. Anal. Calcd for **9**: C, 37.27; H, 4.07; N, 5.79. Found: C, 37.50; H, 3.97; N, 5.66. ^{1}H NMR in $CDCl_3$: δ 2.10 (12H, acetate methyl), 2.17 (12H, acetate methyl), 2.21 (12H, acetate methyl), 2.77 (12H, CNXy methyl), 3.32 (12H, dmap methyl), 7.08−7.23 (6H, isocyanide benzene ring + 4H, dmap-*m*), 9.13 (4H, dmap-*o*), 8.13 (2H, py-*p*), 9.32 (4H, pz). IR (KBr pellet): ν(CN) = 2025 cm^{-1}. FAB MS: *m*/*z* = 1935 (calcd for **9**).

[{Ru$_3$(O)(CH$_3$CO$_2$)$_6$(CNXy)$_2$}$_2$(μ-pz)] (10). To a $CHCl_3$ solution (15 cm^3) of **1** (50 mg, 0.052 mmol) was added pz (2 mg, 0.026 mmol), and the solution was stirred for 1 day, during which time the color changed from blue-green to black. The solution was evaporated to dryness using a rotary evaporator, and the residue was dissolved in a minimal amount of $CHCl_3$. The latter solution was placed on a column packed with silica gel (Wakogel C-200), and $CHCl_3/C_2H_5OH$ (99.0/1.0, v/v) was used as the eluent. The main fraction was collected and evaporated to dryness. The residue was dissolved in a small amount of $CHCl_3$, and excess *n*-hexane was added to the solution. A dark purple precipitate was isolated. Yield: 29 mg (57%). Anal. Calcd for **10**: C, 39.39; H, 3.92; N, 4.31. Found: C, 39.45; H, 3.95; N, 4.31. ^{1}H NMR in $CDCl_3$: δ 2.24 (12H, acetate methyl), 2.26 (24H, acetate methyl), 2.79 (24H, CNXy methyl),7.20−7.26 (12H, CNXy benzene ring), 8.65 (4H, pz). IR (KBr pellet): ν(CN) = 2070 cm^{-1}. FAB MS: *m*/*z* = 1953 (calcd for **10**).

[{Ru$_3$(O)(CH$_3$CO$_2$)$_6$(py)$_2$}$_2$(μ-CNC$_6$H$_4$NC)] (11). To a benzene solution (30 cm^3) of [Ru$_3$(O)(CH$_3$CO$_2$)$_6$(CO)(py)$_2$][30] (200 mg, 0.233 mmol) was added CNC_6H_4NC (15 mg, 0.117 mmol), and the solution was refluxed for 1 day, during which time the color changed from blue to green. The solution was then evaporated to dryness using a rotary evaporator, the residue was dissolved in a minimal amount of $CHCl_3$, and the mixture was filtered. The filtrate was placed on a column packed with silica gel (Wakogel C-200) and using $CHCl_3/C_2H_5OH$ (98.0/2.0, v/v) as the eluent. The main fraction was collected and evaporated to dryness. The residue was dissolved in a small amount of CH_2Cl_2, and excess *n*-hexane was added to the solution. The blue-green precipitate was collected by filtration. Yield: 31 mg (15%). Anal. Calcd for **11**·2H$_2$O: C, 34.18; H, 3.53; N, 4.60. Found: C, 34.33; H, 3.68; N, 4.66. ^{1}H NMR in $CDCl_3$: δ 1.88 (12H, acetate methyl), 2.12 (24H, acetate methyl), 7.84 (4H, CNC_6H_4NC benzene ring), 8.02 (8H, py-*m*), 8.20 (4H, py-*p*), 9.35 (8H, py-*o*). IR (KBr pellet): ν(CN) = 2010 cm^{-1}. FAB MS: *m*/*z* = 1716 (calcd for **11** − py).

[{Ru$_3$(O)(CH$_3$CO$_2$)$_6$(dmap)$_2$}$_2$(μ-CNC$_6$H$_4$NC)] (12). 12 was synthesized by a method similar to that for **11** using [Ru$_3$(O)(CH$_3$CO$_2$)$_6$(CO)(dmap)$_2$][35] in place of [Ru$_3$(O)(CH$_3$CO$_2$)$_6$(CO)(py)$_2$]. Yield: 44%. Anal. Calcd for **12**·3H$_2$O: C, 35.72; H, 4.30; N, 6.94. Found: C, 35.85; H, 4.31; N, 6.97. ^{1}H NMR in $CDCl_3$: δ 1.83 (12H, acetate methyl), 2.08 (24H, acetate methyl), 3.30 (24H, dmap methyl), 7.22 (8H, dmap-*m*), 7.84 (4H, CNC_6H_4NC benzene ring) 9.19 (8H, dmap-*o*). IR (KBr pellet): ν(CN) = 2010 cm^{-1}. FAB MS: *m*/*z* = 1962 (calcd for **12**).

[{Ru$_3$(O)(CH$_3$CO$_2$)$_6$(CNXy)$_2$}$_2$(μ-CNC$_6$H$_4$NC)] (13). To a $CHCl_3$ solution (15 cm^3) of **1** (52 mg, 0.054 mmol) was added CNC_6H_4NC (3 mg, 0.027 mmol), and the solution was stirred for 1 day. During this time, the color changed from blue to green. The solution was evaporated to dryness using a rotary evaporator, and the residue was dissolved in a minimal amount of $CHCl_3$. This was subjected to column chromatography (Bio-Beads S-X3). The main fraction was collected and evaporated to dryness. The residue was dissolved in a small amount of CH_2Cl_2, and excess *n*-hexane was added to the solution. A yellow-green precipitate was isolated. Yield: 33 mg (61%). Anal. Calcd for **13**: C, 40.84; H, 3.83; N, 4.20. Found: C, 40.86; H, 4.20; N, 4.37. ^{1}H NMR in $CDCl_3$: δ 2.17 (12H, acetate methyl), 2.32 (24H, acetate methyl), 2.88 (24H, CNXy methyl), 7.01 (4H, CNXy-*p*), 7.33 (8H, CNXy-*m*), 7.57 (4H, CNC_6H_4NC). IR (KBr pellet): ν(CN) = 2070 cm^{-1}. FAB MS: *m*/*z* = 1737 (calcd for **13** − 2(CNXy)).

Results and Discussion

Preparation of Compounds. Previously, we reported that the carbonyl cluster [Ru$_3$(O)(CH$_3$CO$_2$)$_6$(CO)(L^1)(L^2)] (L^1, L^2 = non-carbonyl ligand) is a convenient starting material for the preparation of various derivatives.[30] The carbonyl ligand site of these clusters is normally substitutionally inert but will undergo elimination under certain conditions to substitute a solvent molecule. The resulting solvent site is labile and readily replaced by stronger ligands such as pyridyl ligands.[8,37]

In the present study, a series of isocyanide complexes, **2**−**13**, were synthesized via the substitution of the carbonyl ligand. The substitutions include not only those for isocyanide ligands but also those for various pyridyl ligands. Compound **1**, which

(37) Sasaki, Y.; Nagasawa, A.; Tokiwa, A.; Ito, T. *Inorg. Chim. Acta* **1993**, *212*, 175−182.

Scheme 1

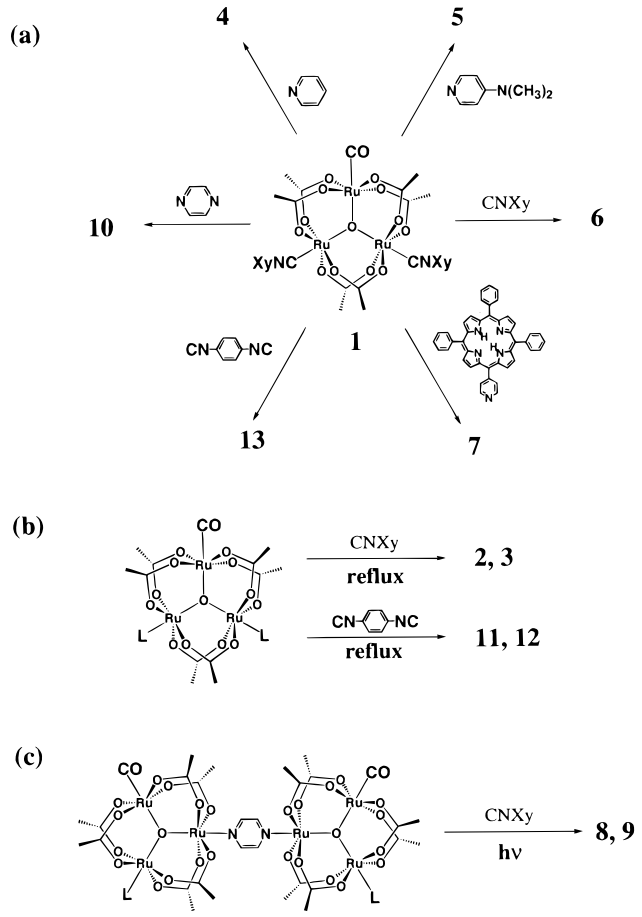

has a terminal CO ligand, is an important starting complex leading to the new derivatives. The reaction of $[Ru_3(O)(CH_3CO_2)_6(CO)(C_2H_5OH)_2]$ with CNXy causes not only substitution of ethanol, which affords $[Ru_3(O)(CH_3CO_2)_6(CO)(CNXy)_2]$ (**1**), but also substitution of the carbonyl ligand, which affords the fully isocyanide-substituted cluster $[Ru_3(O)(CH_3CO_2)_6(CNXy)_3]$ (**6**). Even when exactly 2 equiv of CNXy was used, mostly the trisubstituted complex **6** was obtained. This is because **1** easily eliminates its carbonyl ligand (vide infra). Bubbling CO through the reaction to prevent elimination of the carbonyl ligand decreases the yield of **6** and increases the yield of **1**. However, **6** does not undergo substitution of CNXy upon bubbling CO through the solution.

Scheme 1 summarizes the synthetic routes to the present series of compounds. These are classified into three groups depending on the techniques used for the elimination of the carbonyl ligand.

In Scheme 1a, the substitution of the carbonyl group of **1** by an isocyanide or pyridyl ligand is accomplished simply by stirring a chloroform or dichloromethane solution of **1** in the presence of the desired ligand at room temperature. In Scheme 1b, substitution of the carbonyl ligand by a terminal or bridging isocyanide ligand is achieved by refluxing the reaction mixture. In Scheme 1c, the carbonyl ligands are eliminated by photolysis in the presence of the incoming isocyanide ligand. Compounds **2** and **3** were also obtained by the photosubstitution of the carbonyl ligand. The pyrazine bridged Ru_3 dimers **8** and **9**, however, can only be synthesized via photodecarbonylation because of thermal degradation of the pyrazine bridged Ru_3 dimeric structure to monomeric Ru_3 species.

All of the compounds **1**−**13** are diamagnetic as evidenced by ^{1}H NMR behavior, and all the $Ru_3(O)$ cores have the formal oxidation state of $Ru^{III}_2Ru^{II}$ in the isolated state. It is noteworthy that, although both carbon monoxide and isocyanides are similar π-acid ligands, only one carbonyl ligand can be introduced to the $Ru_3(\mu_3\text{-}O)(CH_3CO_2)_6$ cluster core, whereas the core can accept up to three isocyanides. The complexes with one isocyanide ligand per triruthenium unit were prepared by substitution of a triruthenium carbonyl cluster. The complexes with two isocyanide ligands per triruthenium unit were prepared from the mixed carbonyl−isocyanide complex $[Ru_3(O)(CH_3CO_2)_6(CO)(CNXy)_2]$ (**1**).

Table 2. ν(C≡N) and ν(C≡O) Frequencies (cm^{-1}) of Triruthenium Cluster Monomers

complex		oxidn state[a]	ν-(C≡N)	ν-(C≡O)
$[Ru_3(O)(CH_3CO_2)_6(CO)(py)_2]$	(III,III,II)			1943
$[Ru_3(O)(CH_3CO_2)_6(CNXy)_3]^+$ (**6**$^+$)	(III,III,III)	3.0	2168[b]	
$[Ru_3(O)(CH_3CO_2)_6(CNXy)(py)_2]^+$ (**2**$^+$)	(III,III,III)	3.0	2168[b]	
$[Ru_3(O)(CH_3CO_2)_6(CO)(CNXy)_2]$ (**1**)	(III,III,II)	3.0	2150	1942
$[Ru_3(O)(CH_3CO_2)_6(CNXy)_3]$ (**6**)	(III,III,II)	2.67	2100	
$[Ru_3(O)(CH_3CO_2)_6(CNXy)_2(py)]$ (**4**)	(III,III,II)	2.5	2060	
$[Ru_3(O)(CH_3CO_2)_6(CNXy)(py)_2]$ (**2**)	(III,III,II)	2.0	2015	

[a] Mean oxidation state of ruthenium coordinated by isocyanide. [b] CH_2Cl_2 solution (SEC cell), ref 44.

The methyl isocyanicde complexes $[Ru_3(O)(RCO_2)_6(CH_3NC)_{3-n}(L)_n]$ ($n = 0, 1$) reported by Spencer and Wilkinson have been prepared by substitution reactions of $[Ru_3(O)(RCO_2)_6(CH_3OH)_3]$.[15]

Reactivity of $[Ru_3(O)(CH_3CO_2)_6(CO)(CNXy)_2]$ (1). Competition between Carbonyl and Isocyanide Ligands as π Acids. $[Ru_3(O)(CH_3CO_2)_6(CO)(CNXy)_2]$ (**1**) undergoes elimination of its carbonyl ligand under very mild conditions to give various derivatives (Scheme 1a). In these reactions, the desired products are obtained in high yields by stirring a solution containing **1** with an equimolar amount of the incoming ligand at room temperature. The ease with which the carbonyl ligand in **1** is eliminated is remarkable when compared with the Ru−CO bond cleavage in other triruthenium complexes. This suggests that the Ru atom bound to CO in **1** is in an electronically unusual state. It arises from the simultaneous coordination of CO and CNXy ligands, both of which are π acids, to the $Ru_3(O)(CH_3CO_2)_6$ cluster core.

Table 2 shows the IR absorption frequencies of ν(CN) and ν(CO) for **1** along with those for the related compounds in various oxidation states.

Generally, ν(CN) frequencies of isocyanide complexes are known to be sensitive to the oxidation state of the metal.[38] In fact, ν(CN) data for a series of Ru_3 complexes spread over a relatively wide range. The ν(CO) frequency of **1** (1942 cm^{-1}) is similar to those of other triruthenium clusters with a carbonyl ligand, whereas the ν(CN) frequency of **1** is rather similar to those of the other isocyanide complexes in the Ru^{III}_3 state. This observation suggests that the ruthenium coordinated by CO is essentially divalent as is reported for $[Ru_3O(CH_3CO_2)_6(CO)(mbpy^+)_2](ClO_4)_2\cdot 2DMF$ ($mbpy^+$ = *N*-methyl-4,4′-bipyridinium)[16] and that the ruthenium coordinated by the isocyanides are trivalent. This occurs although both carbonyl and isocyanide ligands can stabilize a divalent ruthenium center. This is caused by the fact that isocyanide ligands have less π-accepting capacity than CO. The ν(CN) band of **1**, however, is shifted slightly to lower energy relative to those of other isocyanide complexes in the Ru^{III}_3 state. This implies a slight decrease in the oxidation state of the ruthenium coordinated by isocyanide ligands and a slight increase in the oxidation state of the ruthenium

(38) Treichel, P. M. *Adv. Organomet. Chem.* **1973**, *11*, 21−86.

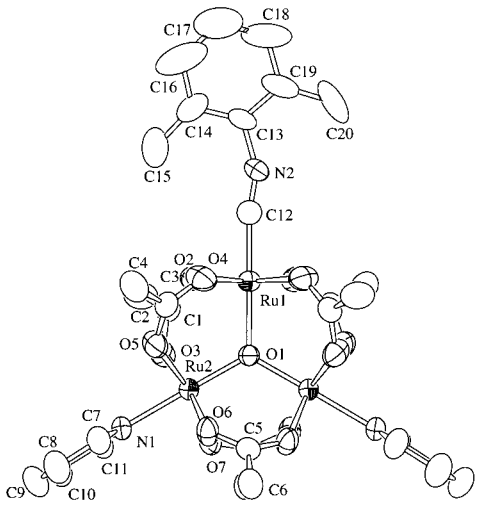

Figure 1. ORTEP drawing of **2** in $[Ru_3(O)(CH_3CO_2)_6(CNXy)(py)_2]\cdot 2CHCl_3$ (**2**·$2CHCl_3$). For clarity, hydrogen atoms are omitted and only one of the two disordered CNXy ligands is depicted.

Table 3. Selected Interatomic Distances (Å) and Bond Angles (deg) for $[Ru_3(O)(CH_3CO_2)_6(CNXy)(py)_2]\cdot 2CHCl_3$ (**2**·$2CHCl_3$)

		Distances	
Ru1−O1	2.035(3)	Ru1−O2	2.085(3)
Ru1−O4	2.061(3)	Ru1−C12	1.880(5)
Ru2−O1	1.888(1)	Ru2−O3	2.038(3)
Ru2−O5	2.044(3)	Ru2−O6	2.047(3)
Ru2−O7	2.045(3)	Ru2−N1	2.139(3)
N2−C12	1.188(7)	N2−C13	1.43(1)
		Angles	
O2−Ru1−C12	87.88(7)	O4−Ru1−C12	87.98(7)
O1−Ru2−N1	178.7(1)	O3−Ru2−N1	86.0(1)
O5−Ru2−N1	84.9(1)	O6−Ru2−N1	86.2(1)
O7−Ru2−N1	83.8(1)	Ru1−C12−N2	169.4(8)
C12−N2−C13	153(2)		

coordinated by CO. This "leaking" of charge off the Ru^{II}−CO site onto the Ru^{III}−CNXy sites may cause a decrease of back-donation to the carbonyl, which weakens the Ru−C bond and causes its facile elimination. The reason the isocyanide ligands of **1** are not eliminated is that they coordinate primarily through a σ interaction.

X-ray Structure of $[Ru_3(O)(CH_3CO_2)_6(CNXy)(py)_2]\cdot 2CHCl_3$ (2·$2CHCl_3$). The ORTEP drawing of **2** is shown in Figure 1. There is a crystallographic 2-fold axis through Ru1−O1, and the CNXy ligand is disordered at two positions related by the C_2 axis with 0.5 occupancy. Selected interatomic distances and bond angles are collected in Table 3.

The triangle formed by the three ruthenium ions is isosceles rather than equilateral. The Ru1···Ru2 distance (3.3909(4) Å) is significantly longer than the Ru2···Ru2′ distances (3.2840(7) Å). This is caused by the lengthening of the Ru1−O1 bond (2.035(3) Å), caused by a trans influence of the CNXy ligand, as compared with the Ru2−O1 bond (1.888(1) Å) (Chart 2). This is similar to the case of the related CO complex $[Ru_3(O)(CH_3CO_2)_6(CO)(mbpy^+)_2](ClO_4)_2\cdot 2DMF$, in which the Ru−O distance at the CO site (2.039(11) Å) is longer than the distance involving the $mbpy^+$ site (1.894(6) Å).[16]

This suggests that the trans influence of the CNXy ligand is similar to that of the CO ligand. A clear difference was found also among the Ru−O(acetate) distances. The Ru1−O(acetate) bonds (2.061(3) and 2.085(3) Å) at the CNXy site are significantly longer than the Ru2−O(acetate) bonds (2.038(3)−2.047(3) Å) at the pyridine site. The CNXy ligand stabilizes the Ru^{II} states similarly to a CO ligand. This is a normal

Chart 2

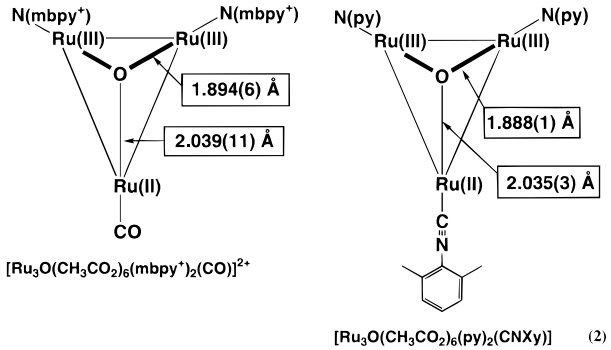

consequence for strong π acceptors, such as CO or isocyanides. Thus, Ru1 bound to the CNXy ligand is formally in the valence-trapped Ru^{II} state while Ru2 and Ru2′, each bound to pyridine, are Ru^{III}.

A notable structural feature is the evidence for π back-bonding. The C12−N2−C13 angle is 153(2)°, which is smaller than the angle expected for a terminal isocyanide ligand with CN triple-bond character (180°). Coupled with the lower energy IR stretch (2015 cm^{-1}), compared to that for free CNXy (2117 cm^{-1}), the decreased angle suggests that there is significant back-donation into the π^* orbital of the CN triple bond, with the CN bond approaching double-bond character.

Electronic Spectra. The triruthenium complexes containing isocyanide ligands generally show three absorption bands. On the basis of band assignments for similar triruthenium complexes,[3] a near-IR absorption band at ca. 600−1000 nm is assigned to an intracluster charge transfer (IC). A low-energy absorption at ca. 300 nm in the UV region is assigned to a cluster to ligand charge-transfer transition (CLCT), and the highest energy band (ca. 250 nm) is assigned to a $\pi-\pi^*$ transition of the ligand. Absorption spectral data for the newly synthesized complexes are summarized in Table 4.

A remarkable feature was observed for the IC bands of a series of isocyanide complexes, $[Ru_3(O)(CH_3CO_2)_6(CNXy)_n(py)_{3-n}]$ ($n = 1$ (**2**), 2 (**4**), 3 (**6**)) (Figure 2).

The absorption spectral pattern in the near-IR region strongly depends on the number of isocyanide ligands, especially for **4**, which shows two separate peaks. Since isocyanide ligands prefer low-valent metal centers, the trivalent rutheniums are coordinated by two pyridines in **2**, formally one pyridine and one isocyanide in **4**, and two isocyanides in **6**. Therefore, the absorption at ca. 600 nm seen for **2** and **4** can be assigned to the transition from the divalent ruthenium to the trivalent ruthenium coordinated by pyridine.

Although the isocyanide and the carbonyl ligands are isoelectronic, the intracluster transition differs slightly between isocyanide and carbonyl complexes. For example, the carbonyl complex $[Ru_3(O)(CH_3CO_2)_6(CO)(py)_2]$[3] shows an absorption peak maximum at 589 nm, while the isocyanide complex **2** shows the corresponding peak maximum at longer wavelength (634 nm) with a shoulder at 745 nm.

Cyclic Voltammetry. Spencer and Wilkinson reported the electrochemistry for the methyl isocyanide comlexes $[Ru_3(O)(RCO_2)_6(CH_3NC)_{3-n}(L)_n]$ ($n = 0, 1$).[15] Redox behaviors of the present series of Ru_3 compounds show, however, much richer electrochemical behaviors than those of methyl isocyanide complexes.[39] All of the present triruthenium complexes with isocyanide ligands were isolated as neutral compounds where each triruthenium cluster core is in the formal oxidation state

Table 4. Absorption Spectral Data for the Monomeric Compounds (**1**−**7**) and Dimeric Compounds (**8**−**13**)

complex	λ_{max} (nm) (ϵ (M^{-1} cm^{-1})) IC	CLCT	$\pi-\pi^*$
$[Ru_3(O)(CH_3CO_2)_6(CO)(CNXy)_2]$ (**1**)	674 (5150)	304 (17 800)	233 (34300)
$[Ru_3(O)(CH_3CO_2)_6(CNXy)(py)_2]$ (**2**)	745 (3920), 634 (4290)	320 (14 000)	247 (28600)
$[Ru_3(O)(CH_3CO_2)_6(CNXy)(dmap)_2]$ (**3**)	625 (6150)	318 (26 400)	261 (39100)
$[Ru_3(O)(CH_3CO_2)_6(CNXy)_2(py)]$ (**4**)	986 (5820), 684 (4530)	317 (19 000)	245 (30000)
$[Ru_3(O)(CH_3CO_2)_6(CNXy)_2(dmap)]$ (**5**)	968 (6250), 678 (7760)	314 (25 700)	254 (35800)
$[Ru_3(O)(CH_3CO_2)_6(CNXy)_3]$ (**6**)	998 (10800)	314 (26 900)	237 (39100)
$[Ru_3(O)(CH_3CO_2)_6(CNXy)_2\{H_2(4\text{-pyp3p})\}]$ (**7**)	984 (6790)	306 (35 200)	241 (49200)
$[\{Ru_3(O)(CH_3CO_2)_6(CNXy)(py)\}_2(pz)]$ (**8**)	834 (12 500), 680 (14 400), 498 (13 000)	318 (31 800)	248 (67 700)
$[\{Ru_3(O)(CH_3CO_2)_6(CNXy)(dmap)\}_2(pz)]$ (**9**)	744 (11 800), 664 (14 900), 498 (11 300)	317 (35 600)	259 (61 900)
$[\{Ru_3(O)(CH_3CO_2)_6(CNXy)_2\}_2(pz)]$ (**10**)	984 (17 700), 762 (16 200)	315 (43 900)	237 (69 700)
$[\{Ru_3(O)(CH_3CO_2)_6(py)_2\}_2(CNC_6H_4NC)]$ (**11**)	707 (8090)	369 (31 700)	248 (47 700)
$[\{Ru_3(O)(CH_3CO_2)_6(dmap)_2\}_2(CNC_6H_4NC)]$ (**12**)	624 (14 500)	383 (40 700), 316 (48 100)	263 (77 200)
$[\{Ru_3(O)(CH_3CO_2)_6(CNXy)_2\}_2(CNC_6H_4NC)]$ (**13**)	1024 (21 500)	357 (39 800), 304 (49 700)	238 (81 400)

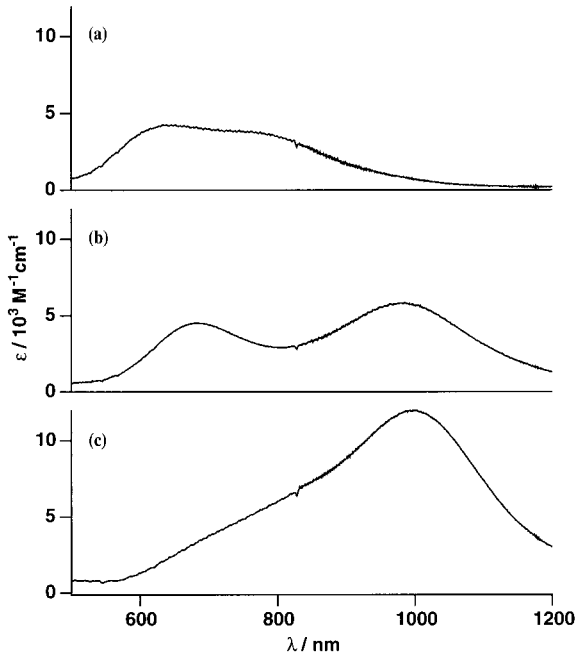

Figure 2. Electronic absorption spectra of (a) $[Ru_3(O)(CH_3CO_2)_6(CNXy)(py)_2]$ (**2**), (b) $[Ru_3(O)(CH_3CO_2)_6(CNXy)_2(py)]$ (**4**), and (c) $[Ru_3(O)(CH_3CO_2)_6(CNXy)_3]$ (**6**) in CH_3CN.

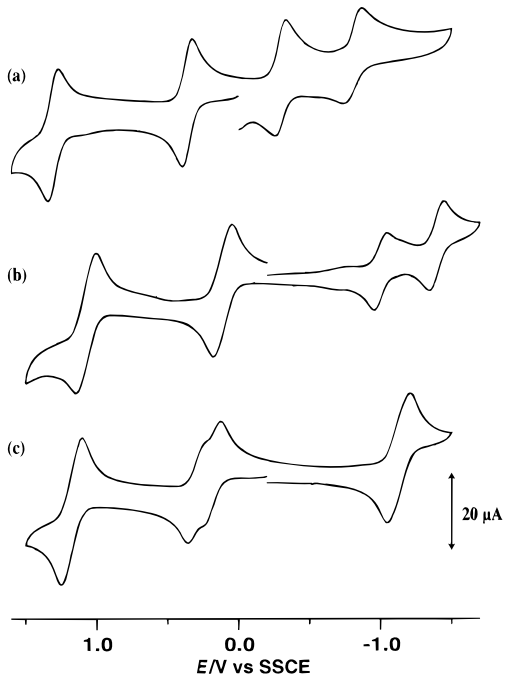

Figure 3. Cyclic voltammograms of (a) the Ru_3 monomer $[Ru_3(O)(CH_3CO_2)_6(CNXy)_3]$ (**6**), (b) the pyrazine bridged Ru_3 dimer $[\{Ru_3(O)(CH_3CO_2)_6(CNXy)(dmap)\}_2(\mu\text{-pz})]$ (**9**), and the 1,4-phenylene diisocyanide bridged Ru_3 dimer $[\{Ru_3(O)(CH_3CO_2)_6(py)_2\}_2(\mu\text{-}CNC_6H_4NC)]$ (**11**) in a 0.1 M $[(n\text{-}C_4H_9)_4N]PF_6-CH_3CN$ (a) or $-CH_2Cl_2$ (b, c) solution. Scan rate = 100 mV s^{-1}.

$Ru^{III}_2Ru^{II}$. The redox potential data for these complexes are summarized in Table 5.

In general, the clusters possess two oxidation processes associated with the Ru_3 core, $Ru^{III}_3/Ru^{III}_2Ru^{II}$ and $Ru^{III}_2Ru^{IV}/Ru^{III}_3$, and one reduction process, $Ru^{III}_2Ru^{II}/Ru^{III}Ru^{II}_2$. A further reversible reduction process, $Ru^{III}Ru^{II}_2/Ru^{II}_3$ is clearly observed only for $[Ru_3(O)(CH_3CO_2)_6(CNXy)_3]$ (**6**). Figure 3 shows cyclic voltammograms of Ru_3 monomer **6**, pyrazine bridged Ru_3 dimer **9**, and 1,4-phenylene diisocyanide bridged Ru_3 dimer **11**, as typical examples.

(a) Ru_3 Monomers. The presence of CNXy ligands profoundly stabilizes the Ru^{II} state within the Ru_3 cores of these complexes. This is well reflected in the comparison of the cyclic voltammetry data for the series of compounds with one CNXy and two dmap ligands (**3**), two CNXy ligands and one dmap ligand (**5**), and three CNXy ligands (**6**) (Table 5).

Two trends are evident. First, as the number of isocyanide ligands increases, the redox potentials shift to more positive potentials. This is an expected result of the isocyanide ligands being weaker electron-donor and stronger π-acceptor ligands compared to pyridyl ligands. Second, the isocyanides significantly lower the Ru^{III}/Ru^{II} formal reduction potentials. In **3**, the CNXy ligand occupies the Ru^{II} site in the isolated state, so the cathodic $Ru^{III}_2Ru^{II}/Ru^{III}Ru^{II}_2$ process must reduce a dmap site, and this occurs at −1.207 V. In **5**, a second CNXy ligand site is available so that the $Ru^{III}_2Ru^{II}/Ru^{III}Ru^{II}_2$ process can occur with a CNXy ligand in each Ru^{II} site. This process now occurs at −0.505 V, reflecting the significant stabilization of Ru^{II} by an isocyanide compared to a pyridyl ligand. In the triisocyanide complex **6**, the third isocyanide ligand further shifts the $Ru^{III}_2Ru^{II}/Ru^{III}Ru^{II}_2$ process to more positive potentials, and the $Ru^{III}Ru^{II}_2/Ru^{II}_3$ process is now observed as a reversible wave (Figure 3a). Compounds **3** and **5** never show a well-defined reversible wave for the $Ru^{III}Ru^{II}_2/Ru^{II}_3$ process (Table 5). A similar positive

(39) Spencer and Wilkinson reported, for example, that $[Ru_3(O)(CH_3CO_2)_6(CH_3NC)_3]$ shows $1e^-$ oxidation and irreversible $2e^-$ reduction waves in dimethylacetamide. Such behavior is not consistent with the general electrochemical behavior of the present isocyanide Ru_3 complexes.

Table 5. Electrochemical Data for the Monomeric Compounds (**1**−**7**), Dimeric Compounds (**8**−**13**), and Related Compounds

	$E_{1/2}$ (V[a]) (*n*e[b])			
complex	(III,III,IV)/(III,III,III)	(III,III,III)/(III,III,II)	(III,III,II)/(III,II,II)	(III,II,II)/(II,II,II)
$[Ru_3(O)(CH_3CO_2)_6(CO)(dmap)_2]$	1.10 (1e)	0.54 (1e)	−1.08 (1e)	−2.03[e] (1e)
$[Ru_3(O)(CH_3CO_2)_6(CO)(py)_2]$[c]	1.27 (1e)	0.62 (1e)	−0.90 (1e)	−1.76[e] (1e)
$[Ru_3(O)(CH_3CO_2)_6(CO)(CNXy)_2]$ (**1**)[d]	1.50 (1e)	0.69 (1e)	−0.13 (1e)	−0.73 (1e)
$[Ru_3(O)(CH_3CO_2)_6(CNXy)(py)_2]$ (**2**)	1.11 (1e)	0.26 (1e)	−1.00 (1e)	−1.80[e] (1e)
$[Ru_3(O)(CH_3CO_2)_6(CNXy)(dmap)_2]$ (**3**)	0.95 (1e)	0.16 (1e)	−1.21 (1e)	
$[Ru_3(O)(CH_3CO_2)_6(CNXy)_2(py)]$ (**4**)	1.21 (1e)	0.31 (1e)	−0.45 (1e)	−1.50[e] (1e)
$[Ru_3(O)(CH_3CO_2)_6(CNXy)_2(dmap)]$ (**5**)	1.10 (1e)	0.27 (1e)	−0.51 (1e)	−1.80[e] (1e)
$[Ru_3(O)(CH_3CO_2)_6(CNXy)_3]$ (**6**)	1.31 (1e)	0.36 (1e)	−0.30 (1e)	−0.82 (1e)
$[Ru_3(O)(CH_3CO_2)_6(CNXy)_2\{H_2(4\text{-}pyp3p)\}]$ (**7**)		0.18 (1e)	−0.65 (1e)	
$[\{Ru_3(O)(CH_3CO_2)_6(CNXy)(py)\}_2(pz)]$ (**8**)	1.15 (2e)	0.14 (2e)	−0.96 (1e), −1.31 (1e)	
$[\{Ru_3(O)(CH_3CO_2)_6(CNXy)(dmap)\}_2(pz)]$ (**9**)	1.07 (2e)	0.11 (2e)	−1.00 (1e), −1.39 (1e)	
$[\{Ru_3(O)(CH_3CO_2)_6(CNXy)_2\}_2(pz)]$ (**10**)	1.26 (2e)	0.22 (2e)	−0.57 (1e), −0.65 (1e)	−1.42[e] (1e), −1.67[e] (1e)
$[\{Ru_3(O)(CH_3CO_2)_6(py)_2\}_2(CNC_6H_4NC)]$ (**11**)	1.15 (2e)	0.28 (1e), 0.17 (1e)	−1.15 (2e)	
$[\{Ru_3(O)(CH_3CO_2)_6(dmap)_2\}_2(CNC_6H_4NC)]$ (**12**)	0.99 (2e)	0.16 (1e), 0.02 (1e)	−1.43 (2e)	
$[\{Ru_3(O)(CH_3CO_2)_6(CNXy)_2\}_2(CNC_6H_4NC)]$ (**13**)	1.30 (2e)	0.26 (2e)	−0.44 (1e), −0.51 (1e)	−1.05[e] (2e)

[a] vs SSCE. [b] *n*e = number of electrons exchanged. [c] Reference 3. [d] See ref 40. [e] Irreversible.

shift was observed for the series of complexes containing pyridine, $[Ru_3(O)(CH_3CO_2)_6(CNXy)_n(py)_{3-n}]$ ($n = 1$ (**2**), 2 (**4**), 3 (**6**)).

When CV data for $[Ru_3(O)(CH_3CO_2)_6(CNXy)(dmap)_2]$ (**3**) and $[Ru_3(O)(CH_3CO_2)_6(CO)(dmap)_2]$ are compared, the corresponding redox couples are observed at more positive potentials for the carbonyl complex than for the isocyanide complex **3**, suggesting that the carbonyl is more electron withdrawing (Table 5). The difference in $E_{1/2}$ for the $Ru^{III}_3/Ru^{III}_2Ru^{II}$ process is particularly large ($E_{1/2} = +0.161$ V for **3** and +0.537 V for the carbonyl complex). This shows a clear difference between these two ligands in giving rise to a Ru^{III} state. The formation of a $Ru^{III}-CO$ bond is far more difficult compared to $Ru^{III}-CNXy$ bond formation. A similar large difference in $E_{1/2}$ for the $Ru^{III}_3/Ru^{III}_2Ru^{II}$ process can be seen in a comparison of the diisocyanide monocarbonyl $[Ru_3(O)(CH_3CO_2)_6(CO)(CNXy)_2]$ (**1**) (+0.690 V) and the triisocyanide complex $[Ru_3(O)(CH_3CO_2)_6(CNXy)_3]$ (+0.362 V). This is due to the same effect.

(b) Bridged Ru_3 Dimers. The CV patterns of the pyrazine bridged dimers, $[\{Ru_3(O)(CH_3CO_2)_6(CNXy)(L)\}_2(\mu\text{-pz})]$ (L = py (**8**), L = dmap (**9**)), are very similar to each other (Table 5 and Figure 3b) and are very similar also to those of the carbonyl derivatives $[\{Ru_3(O)(CH_3CO_2)_6(CO)(L)\}_2(\mu\text{-pz})]$ (L = dmap, py, cpy).[31] The redox behavior of the carbonyl derivatives have been fully elucidated in our previous study, and the redox waves of **8** and **9** are assigned as given in Table 5. Each of complexes **8** and **9** shows two single-electron-reduction waves around −1.0 and −1.3 V vs SSCE that correspond to $Ru^{III}_2Ru^{II}-pz-Ru^{III}_2Ru^{II}/Ru^{III}_2Ru^{II}-pz-Ru^{III}Ru^{II}_2$ (0/−1) and then $Ru^{III}_2Ru^{II}-pz-Ru^{III}Ru^{II}_2/Ru^{III}Ru^{II}_2-pz-Ru^{III}Ru^{II}_2$ (−1/−2). Here the overall charges of the complexes are expressed in parentheses. The splitting between the (0/−1) and (−1/−2) states is 349 mV for **8** and 393 mV for **9**. One important contribution to the magnitude of the splitting between the single-electron-reduction waves, ΔE, is the stabilization energy imparted to the −1 state by electron delocalization,[41,42] and ΔE is related to a comproportionation constant (K_c) as

$$K_c = \exp(\Delta EF/RT)$$

Therefore the magnitude of ΔE (or K_c) shows the stability of the −1 state, which is a mixed-valence state between Ru_3 units. The observed values of $\Delta E = 349$ mV ($K_c = 8.1 \times 10^5$) for $\mathbf{8}^-$ and 393 mV (4.5×10^6) for $\mathbf{9}^-$ are slightly smaller than those for corresponding carbonyl complexes (380 mV (2.7×10^6) and 440 mV (2.7×10^7) for $[\{Ru_3(O)(CH_3CO_2)_6(CO)(L)\}_2(\mu\text{-pz})]$ (L = py and dmap), respectively). The ΔE and K_c values for $\mathbf{8}^-$ and $\mathbf{9}^-$ are, however, by far larger than those reported for the corresponding mixed valence states of analogous Ru_3 dimers that do not bear the CO ligand.[27,28] This shows that the isocyanide ligand, like CO, gives rise to stable mixed-valence species, $\mathbf{8}^-$ and $\mathbf{9}^-$.

There are two main factors that govern the magnitude of ΔE for this type of Ru_3 dimer. One is a distance between communicating centers. The shorter the distance, the stronger the electronic interaction, if the degree of π conjugation is the same. This factor is related to which Ru atom in the $Ru_3(O)$ core accepts an electron upon reduction. It has been shown that the $Ru_3(O)$ core has delocalized electronic structure to form π MO's.[3] And the contributions of the Ru atoms in the $Ru_3(O)$ core to the π MO[43] to which the electron is added are not the same and depend on the nature of the terminal ligand. When the bridging Ru site is bound to the most electronegative ligand and thereby accepts the electorn mainly, the distance will be the shortest, giving a large ΔE. The other is energy match of levels between the π MO of the Ru_3 core and the bridging ligand π^* orbital through which electronic communication is mediated. The closer the two levels, the more easily the inter-Ru_3-unit interaction is mediated. It has been shown for carbonyl Ru_3 dimers, $[\{Ru_3(O)(CH_3CO_2)_6(CO)(L)\}_2(\mu\text{-pz})]$ (L = dmap, py, cpy), that the two levels become closer on going from cpy, py to dmap.[31] The relative magnitude of ΔE for this type of Ru_3 dimer can be explained qualitatively in terms of these two factors.

The smaller ΔE for isocyanide dimers **8** and **9** compared to the corresponding carbonyl dimers $[\{Ru_3(O)(CH_3CO_2)_6(CO)(L)\}_2(\mu\text{-pz})]$ originates from less π acidity of CNXy. This causes the less contribution of the bridging Ru atom to the MO in the CNXy complexes. The difference in ΔE between **8** (349 mV) and **9** (393 mV) as well as the difference in mean $E_{1/2}$ [$=^1/_2$-

(40) This compound is unstable in CH_3CN (see text). Its time-dependent cyclic voltammogram shows decrease of the waves of **1** and increase of waves of the decarbonylated species, probably $[Ru_3(O)(CH_3CO_2)_6(CNXy)_2(CH_3CN)]$.

(41) Richardson, D. E.; Taube, H. *Coord. Chem. Rev.* **1984**, *60*, 107−129.

(42) Richardson, D. E.; Taube, H. *Inorg. Chem.* **1981**, *20*, 1278−1285.

(43) This level corresponds to the Ru−(μ_3-O) antibonding orbital, i.e., the highest level in Meyer's MO scheme,[3] though the symmetry of the $Ru_3(O)$ core in compounds of this study is lowered.

$\{E_{1/2}\ (0/-1) + E_{1/2}\ (-1/-2)\}$] between **8** (−1.13 V) and **9** (−1.20 V) arises from the difference in pK_a for dmap and py, as in the corresponding carbonyl complexes [{$Ru_3(O)(CH_3CO_2)_6(CO)(L)\}_2(\mu$-pz)] (L = py, dmap).[31] The larger pK_a of dmap makes the π^* MO level of the $Ru_3(O)$ core higher, thereby making the reduction more difficult, and at the same time causes the $Ru_3(O)$ MO level to be closer to the pyrazine π^* level.

The rather large ΔE and K_c for $\mathbf{8}^-$ and $\mathbf{9}^-$ prompted us to estimate the rate of intramolecular electron transfer in the Ru_3 unit through bridging pyrazine in $\mathbf{8}^-$ and $\mathbf{9}^-$ in the same way as was done successfully in our previous study.[31] We expected, in view of the large ΔE and K_c values, that the ν(CN) IR band, which is normally sharp, might broaden for $\mathbf{8}^-$ and $\mathbf{9}^-$, if intramolecular electron transfer occurs near the IR time scale as it does in the carbonyl complexes. We surely observed significant line broadening for both $\mathbf{8}^-$ and $\mathbf{9}^-$ by IR spectroelectrochemistry. However, much of the line broadening in these isocyanide systems is attributed to Fermi resonances, which complicate the ν(CN) IR band shape. Therefore, it was not possible to estimate the intramolecular electron-transfer rate constants for $\mathbf{8}^-$ and $\mathbf{9}^-$ by this means. Details of the Fermi resonances observed for the present series of isocyanide complexes are discussed in a separate paper.[44]

The pyrazine bridged dimer [{$Ru_3(O)(CH_3CO_2)_6(CNXy)_2\}_2(\mu$-pz)] (**10**) shows relatively small splitting between the (0/−1) and (−1/−2) processes (ΔE = 88 mV), suggesting that the mixed-valence $\mathbf{10}^-$ state is significantly less stable than $\mathbf{8}^-$ and $\mathbf{9}^-$. In **10**, two terminal sites in each Ru_3 unit are occupied by electron-withdrawering isocyanide ligands, and therefore the electron density in each $Ru_3(O)$ core decreases. This causes a lowering of π MO levels of the cluster core to make the interaction with pyrazine π^* levels less effective.

The 1,4-phenylene diisocyanide bridged dimers, [{$Ru_3(O)(CH_3CO_2)_6(L)_2\}_2(\mu$-$CNC_6H_4NC$)] (L = py (**11**), dmap (**12**)), exhibit four redox waves in the accessible potential region (Table 5, Figure 3c), and their redox potentials are very similar to those for the corresponding pyrazine bridged dimer [{$Ru_3(O)(CH_3CO_2)_6(py)_2\}_2(\mu$-pz)]$(PF_6)_2$. For the pyrazine bridged complex, the redox behavior, including the redox wave assignments, and the origin of the wave splittings have been reported.[27,28] From the similarity of the redox behaviors, each of the CV waves of **11** and **12** was assigned to the same process as that of the pyrazine bridged Ru_3 dimer (Table 5). It should be pointed out that, for **11** and **12**, the redox wave splitting is observed for the process $Ru^{III}{}_3-CNC_6H_4NC-Ru^{III}{}_3/Ru^{III}{}_3-CNC_6H_4NC-Ru^{III}{}_2Ru^{II}/Ru^{III}{}_2Ru^{II}-CNC_6H_4NC-Ru^{III}{}_2Ru^{II}$ (ca. +0.20 V, ΔE = 108 mV for **11** and ca. +0.10 V, ΔE = 141 mV for **12**), whereas the $Ru^{III}{}_2Ru^{II}-CNC_6H_4NC-Ru^{III}{}_2Ru^{II}/Ru^{III}Ru^{II}{}_2-CNC_6H_4NC-Ru^{III}Ru^{II}{}_2$ process ($E_{1/2}$ = −1.149 V for **11** and −1.434 V for **12**) shows no splitting. This presents a striking contrast to the general observation that the magnitude of redox wave splitting for pyrazine bridged dimers with pyridyl terminal ligands increases in a process at a more negative potential region.[27,28] In this case, the bridging CNC_6H_4NC ligand is the most electron withdrawing, and as a result the electron introduced by the reduction would be localized at the bridging Ru site almost completely. The π MO involved in electrocommunication consists, therefore, of d_π of the bridging Ru and π^* of CNC_6H_4NC. The $Ru^{III}{}_2Ru^{II}-CNC_6H_4NC-Ru^{III}{}_2Ru^{II}/Ru^{III}Ru^{II}{}_2-CNC_6H_4NC-Ru^{III}Ru^{II}{}_2$ process shows no redox wave splitting, suggesting that reduction occurs at the nonbridging Ru site.

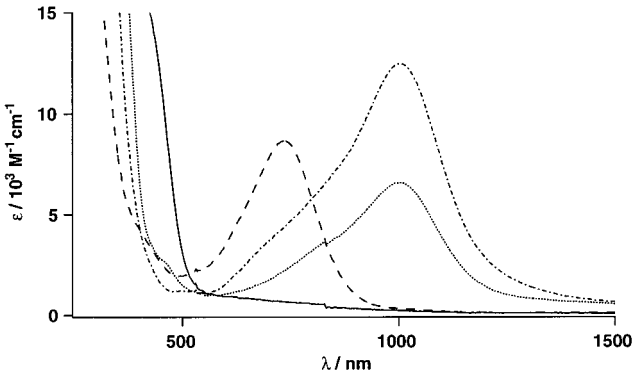

Figure 4. Controlled-potential absorption spectra of [$Ru_3(O)(CH_3CO_2)_6(CNXy)_3$] (**6**) in a 0.1 M [$(n$-$C_4H_9)_4N]PF_6-CH_3CN$ solution: (a) dashed line, 0.84 V; (b) dashed−dotted line, 0 V; (c) dotted line, −0.55 V; (d) solid line, −1.3 V vs SSCE.

The redox behavior of **13**, where all the terminal ligands are electron withdrawring isocyanides, can be understood by similarly considering the two factors given for **8**−**10**.

Spectroelectrochemistry. [$Ru_3(O)(CH_3CO_2)_6(CNXy)_3$] (**6**) exhibits a four-step redox behavior (Figure 3a). The $Ru^{II}{}_3$ state is also stable for this cluster (vide supra), unlike the other triruthenium clusters. The electronic spectra of **6** were measured by use of an OTTLE cell in four redox states from $Ru^{III}{}_3$ to $Ru^{II}{}_3$. Spectra due to the IC transition at 0.84 V ($Ru^{III}{}_3$ state), 0 V ($Ru^{III}{}_2Ru^{II}$ state), −0.55 V ($Ru^{III}Ru^{II}{}_2$ state), and −1.3 V vs SSCE ($Ru^{II}{}_3$ state) are shown in Figure 4.

The absorption band position largely depends on the redox state. The $Ru^{III}{}_3$ state in which all rutheniums are trivalent shows a peak at 734 nm. On the other hand, the mixed-valence states $Ru^{III}{}_2Ru^{II}$ and $Ru^{III}Ru^{II}{}_2$ have absorption maxima at 1004 and 1002 nm, respectively. In the fully reduced $Ru^{II}{}_3$ state, the spectrum shows no peak in the visible to near-IR region. The disappearance of the absorption band in the $Ru^{II}{}_3$ state can be understood by the MO diagram for the $Ru_3(O)$ core proposed by Meyer.[3] In the $Ru^{II}{}_3$ state, all of the molecular orbitals are occupied and no transition can take place among the MO levels. Similar disappearances of absorption bands in the vis−NIR region have been reported for $[Rh_3^{III,III,III}(O)(CH_3CO_2)_6(py)_3]^+$ [45] and $[Ru^{II}{}_3(O)(CH_3CO_2)_6(\text{isonicotinamide})_3]^{2-}$,[18] where all the levels of the MO for $M_3(\mu_3$-O) are fully occupied. It was reported recently that a one-electron-oxidation product of the Rh_3 complex shows an absorption band at 764 nm (ϵ = 4320 M^{-1} cm^{-1}).[46] This supports also the origin of the absorption band of the Ru_3 cluster complexes in the vis−NIR region.

Acknowledgment. This work was supported by Grants-in-Aid for Scientific Research (No. 10740299; the Priority Area "Metal Assembled Complexes" No. 10149102 and an International Scientific Research Program Grant-in-Aid (No. 09044054) from the Ministry of Education, Science, Sports, and Culture of Japan. C.P.K. gratefully acknowledges support from the National Science Foundation (Grant CHE-9615886). We thank Mr. Brian Breedlove for assistance in preparing the manuscript.

Supporting Information Available: An X-ray crystallographic file in CIF format. This material is available free of charge via the Internet at http://pubs.acs.org.

IC990234N

(44) Zavarine, I. S.; Richmond, T.; Kubiak, C. P.; Ota, K.; Hamaguchi, T.; Yamaguchi, T.; Ito, T. Unpublished results.

(45) Sasaki, Y.; Tokiwa, A.; Ito, T. *J. Am. Chem. Soc.* **1987**, *109*, 6341−6347.

(46) Takahashi, K.; Umakoshi, K.; Kikuchi, A.; Sasaki, Y.; Tominaga, M.; Taniguchi, I. *Z. Naturforsch., B* **1995**, *50B*, 551−557.